

Uranyl Complexes with Diamide Ligands: A Quantum Mechanics Study of Chelating Properties in the Gas Phase

Bernard Coupez and Georges Wipff*

Laboratoire MSM, UMR CNRS 7551, Institut de Chimie, 4, rue B. Pascal,
67 000 Strasbourg, France

Received January 31, 2003

We report a quantum mechanical study on the complexes of UO_2^{2+} with diamide ligands L of malonamide and succinamide type, respectively, forming 6- and 7-chelate rings in their bidentate coordination to uranium. The main aims are to (i) assess how strong the chelate effect is (i.e., the preference for bi- versus monodentate binding modes of L), (ii) compare these ligands as a function of the chelate ring size, and (iii) assess the role of neutralizing counterions. For this purpose, we consider UO_2L^{2+} , $\text{UO}_2\text{L}_2^{2+}$, $\text{UO}_2\text{L}_3^{2+}$, and $\text{UO}_2\text{X}_2\text{L}$ type complexes with $\text{X}^- = \text{Cl}^-$ versus NO_3^- . Hartree–Fock and DFT calculations lead to similar trends and reveal the importance of saturation and steric repulsions (“strain”) in the first coordination sphere. In the unsaturated UO_2L^{2+} , $\text{UO}_2\text{L}_2^{2+}$, and $\text{UO}_2\text{Cl}_2\text{L}$ complexes, the 7-ring chelate is preferred over the 6-ring chelate, and bidentate coordination is preferred over the monodentate one. However, in the saturated $\text{UO}_2(\text{NO}_3)_2\text{L}$ complexes, the 6- and 7-chelating ligands have similar binding energies, and for a given ligand, the mono- and bidentate binding modes are quasi-isoenergetic. These conclusions are confirmed by the calculations of free energies of complexation in the gas phase. In condensed phases, the monodentate form of $\text{UO}_2\text{X}_2\text{L}$ complexes should be further stabilized by coordination of additional ligands, as well as by interactions (e.g., hydrogen bonding) of the “free” carbonyl oxygen, leading to an enthalpic preference for this form, compared to the bidentate one. We also considered an isodesmic reaction exchanging one bidentate ligand L with two monoamide analogues, which reveals that the latter are clearly preferred (by 23–14 kcal/mol at the HF level and 24–12 kcal/mol at the DFT level). Thus, in the gas phase, the studied bidentate ligands are enthalpically disfavored, compared to bis-monodentate analogues. The contrast with trends observed in solution hints at the importance of “long range” forces (e.g., second shell interactions) and entropy effects on the chelate effect in condensed phases.

1. Introduction

The chelate effect, i.e., the enhanced stability of a complex containing chelate rings as compared to the stability of a system that is as similar as possible but contains no or fewer rings, is very important in metal coordination chemistry.¹ Many studies have been conducted on first-row transition metal complexes of polyamines, for which 5-membered chelate rings are generally preferred.^{2–6} In the case of actinide or lanthanide complexation, smaller rings are also favored

over larger ones.^{7–11} For instance, diamide ligands of malonamide and succinamide type form strong complexes with $\text{Eu}(\text{ClO}_4)_3$ in an acetonitrile–DMSO mixed solvent,¹² and the resulting EuL_3^{3+} complexes are slightly more stable with malonamide than with succinamide ligands. Similarly, the UO_2^{2+} extraction by a series of symmetrical diamide ligands of $[(\text{C}_4\text{H}_9)_2\text{NCO}]_2(\text{CH}_2)_n$ type ($n = 0, 1, 2$) peaks at $n = 1$, i.e., for a 6-chelate ring.⁸ Malonamides also extract UO_2^{2+} , Nd^{3+} , and Th^{4+} in conditions where succinamides

* To whom correspondence should be addressed. E-mail: wipff@chimie.u-strasbg.fr.

- (1) Cotton, F. A.; Wilkinson, G. *Advanced Inorganic Chemistry*; Wiley: New York, 1988.
- (2) Schwarzenbach, G. *Helv. Chim. Acta* **1952**, *35*, 2344.
- (3) Myers, R. T. *Inorg. Chem.* **1978**, *17*, 952–958.
- (4) Hancock, R. D. *J. Chem. Educ.* **1992**, *69*, 615–621.
- (5) Simmons, E. L. *J. Chem. Educ.* **1979**, *56*, 578.
- (6) Cotton, F. A.; Harris, F. E. *J. Phys. Chem.* **1956**, *60*, 1451.

- (7) Edwards, H. G. M.; Hickmott, E.; Hughes, M. A. *Spectrochim. Acta* **1997**, *A53*, 43–53.
- (8) Choppin, G. R.; Morgenstern, A. *Solvent Extract. Ion Exch.* **2000**, *18*, 1029–1049.
- (9) Barthelemy, P. P.; Choppin, G. R. *Inorg. Chem.* **1989**, *28*, 3354.
- (10) Choppin, G. R. *J. Alloys Compd* **1997**, *249*, 1–8.
- (11) Rozen, A. M. *J. Radioanal. Nucl. Chem.* **1990**, *143*, 337–355.
- (12) Rao, L.; Zanonato, P.; Bernardo, P. D.; Bismondo, A. *Inorg. Chim. Acta* **2000**, *306*, 49–64.

and glutaramides are unsuccessful.⁷ The dicarboxylate $[\text{CO}_2^-]_2(\text{CH}_2)_n$ analogues of diamides also form bidentate complexes with Eu^{3+} in aqueous solution, and their stabilities decrease with larger ligands, i.e., in the order oxalate ($n = 0$) \gg malonate ($n = 1$) $>$ succinate ($n = 2$).^{9,10,13} Similar trends have been observed in the formation of NpO_2^{2+} complexes.¹⁴ Bifunctional di-oxygen ligands may also be used as synergistic agents in liquid–liquid extraction, and size effects have been noticed. For instance, rare earth extraction by alkylsalicylic acids in the presence of diamides, diphosphonates, and disulfoxides as synergistic agents reveals higher synergism when the ligands allow for the formation of a 6-membered instead of 7-membered ring.¹⁵ The interpretation of the chelate effect at the molecular level and the general preference for smaller rings remains a difficult task, due to the interplay between intrinsic interactions in the first coordination sphere (related to the number, size, and conformation of chelate rings, metal–ligand bond properties, and repulsions between the complexed ligands) and changes in solvation properties. Enhanced stabilization may come from the closeness of the other ligand atom(s) once the first ligand bond is formed,^{2,16} from the reduced strain in the first coordination sphere,^{4,17} and from a confluence of several large opposing enthalpic and entropic effects.^{3,18–20} Generally speaking, bidentate coordination of longer ligands suffers an entropy penalty, compared to the shorter ligands, due to the greater loss of internal degrees of freedom,²⁰ but there is so far no direct energy comparison of the two binding modes of a given polyfunctional ligand.

What happens in the gas phase (i.e., in the absence of solvent or environment) may serve as a reference to better understand what happens in condensed phases (solution or solid state). This led us to undertake quantum mechanics (QM) studies on the interaction of M^{3+} lanthanide cations with di-oxygen ligands L bearing different combinations of amide and phosphoryl functionalities, comparing the mono- versus bidentate binding modes of these ligands in MX_3L complexes.^{21–23} In this paper, we report a QM investigation of UO_2^{2+} with two types of diamide ligands, namely N,N,N',N' -tetramethylmalonamide and N,N,N',N' -tetramethylsuccinamide (noted in short AcA and AccA, where c and cc correspond to the CH_2 spacers between the two amide (A) groups; see Figure 1), which, respectively, form 6- and 7-membered rings in their bidentate coordination mode. When compared to M^{3+} lanthanide or actinide ions com-

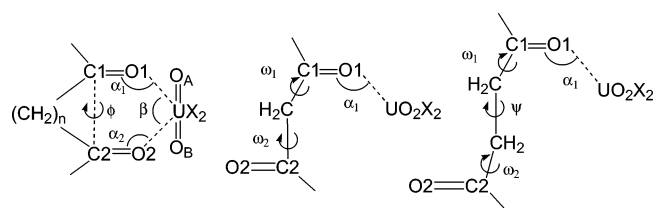


Figure 1. Definition of the structural parameters with AcA ($n = 1$) and AccA ($n = 2$) ligands.

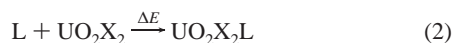
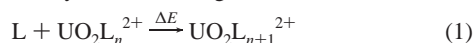
plexes, uranyl complexes display a number of specific features: (i) due to the linear shape of uranyl, the coordination of ligands or anions is restricted to its equatorial plane, perpendicular to the $\text{O}=\text{U}=\text{O}$ axis, and is therefore stereochemically more demanding; (ii) the equatorial coordination number CN of the U atom is low (generally 5 or 6) compared to the CN of M^{3+} cations,²⁴ therefore enhancing the corresponding “steric repulsions” in the first coordination sphere of the metal; (iii) the total +2 charge of uranyl is formally lower than the +3 charge of lanthanide, therefore reducing the metal–ligand electrostatic attractions, an effect which may be compensated by the following feature; (iv) its ionic radius (0.73 Å) is smaller than that of lanthanides (1.15–0.86 Å).²⁵ There are X-ray structures of 1:1 complexes of $\text{UO}_2(\text{NO}_3)_2$ with AcA²⁶ and with an AccA analogue (N,N,N',N' -tetra- n -butylsuccinamide),²⁷ in which the ligand is bidentate. IR spectra of malonamide complexes suggest that similar 1:1 bidentate complexes form in solution.^{26,28,29} However, with noncoordinating or weakly coordinating counterions (e.g., BF_4^- , PF_6^- , ClO_4^- or OTf^-), or at a ligand–metal ratio larger than 2, other species (e.g., of $\text{UO}_2(\text{AcA})_2^{2+}$ type) may also form.²⁶ We thus want to compare the binding energies of AcA versus AccA ligands, as well as the energy difference between their bi- and monodentate binding modes. We first consider 1:1 complexes of UO_2L^{2+} type without counterions, where only one bidentate ligand interacts with UO_2^{2+} . The effect of cumulated ligands is then studied in $\text{UO}_2\text{L}_2^{2+}$ and $\text{UO}_2\text{L}_3^{2+}$ complexes that model complexation without anions in the first coordination sphere. In order to gain insights into the effect of coordinating counterions, we then consider $\text{UO}_2\text{X}_2\text{L}$ complexes bearing two X^- counterions (NO_3^- or Cl^-) equatorially coordinated to uranyl and compare the bi- versus monodentate binding modes of L. The NO_3^- counterions, present in nuclear waste solutions that are obtained by dissolving irradiated fuel in concentrated nitric acid, are found to bidentately coordinate the metal in solid state structures.^{26,27} These are compared with Cl^- counterions which are somewhat more bulky than oxygen binding sites but cannot be bidentate.

- (13) Niu, C.; Choppin, G. *Inorg. Chim. Acta* **1987**, *131*, 277–280.
 (14) Stout, B. E.; Caceci, M. S.; Nectoux, F.; Pages, M. *Radiochim. Acta* **1989**, *46*, 181–184.
 (15) Preston, J. S.; du Preez, A. C. *Solvent Extract. Ion Exch.* **1998**, *16*, 687–706.
 (16) Rosseinsky, D. R. *J. Chem. Soc., Dalton Trans.* **1979**, 732.
 (17) Boeyens, J. C. A.; Comba, P. *Coord. Chem. Rev.* **2001**, *212*, 3–10.
 (18) Hancock, R. D. *Prog. Inorg. Chem.* **1989**, *37*, 187–291.
 (19) Martell, A. E.; Hancock, R. D.; Motekaitis, R. J. *Coord. Chem. Rev.* **1994**, *133*, 39–65 and references therein.
 (20) Chung, C.-S. *J. Chem. Educ.* **1992**, *61*, 1062–1064.
 (21) Boehme, C.; Wipff, G. *Inorg. Chem.* **2002**, *42*, 727–737.
 (22) Boehme, C.; Coupez, B.; Wipff, G. *J. Phys. Chem. A* **2002**, *106*, 6487–6498.
 (23) Coupez, B.; Boehme, C.; Wipff, G. *Phys. Chem. Chem. Phys.* **2002**, *4*, 5716–5729.

- (24) Tabushi, I.; Kokube, Y. *Nippon Kaisui Gakkaishi* **1982**, *36*, 205–217.
 (25) Marcus, Y. *Ion Solvation*; Wiley: Chichester, U.K., 1985.
 (26) Lumetta, G.; McNamara, B. K.; Rapko, B. M.; Sell, R. L.; Rogers, R. D.; Broker, G. A.; Hutchinson, J. E. *Inorg. Chim. Acta* **2000**, *309*, 103–108.
 (27) Wang, H.-Z.; Cui, L.; Cao, Z.-B.; Gu, J.-S.; Zhu, L.-M. *Acta Chim. Sin. (Chinese Edition)* **1993**, *51*, 880.
 (28) Nigond, L.; Musikas, C.; Cuillerdier, C. *Solvent Extract. Ion Exch.* **1994**, *12*, 297–323.
 (29) Ruikar, P. B.; Nagar, M. S. *Polyhedron* **1995**, *14*, 3125.

2. Methods

All compounds were fully optimized by quantum mechanical calculations at the Hartree–Fock (HF) level of theory, using the Gaussian98 software.³⁰ The H, C, N, O, and Cl atoms were described by the 6-31G* basis set.³⁰ For uranium, we used a relativistic large core effective core potential (ECP) of the Los Alamos group³¹ with 78 electrons in the core and a [3s,3p,2d,2f] contracted valence basis set. This level of theory is sufficient to gain insights into energy and structural features of ligand binding to uranyl.^{32,33} Some tests are reported using the Stuttgart ECPs with 60 electrons in the core.^{34,35} The $\text{UO}_2\text{X}_2\text{L}$ and $\text{UO}_2\text{L}_n^{2+}$ complexes were verified as true minima on the potential hypersurface by the analytical calculation of their force constants. All interaction energies ΔE of the ligand L (definition in eqs 1–3) have been corrected for basis set superposition errors (BSSEs),³⁶ which turned out to be small and nearly constant for a given coordination number.



The contribution of harmonic vibration motions to the free energies was also calculated for the $\text{UO}_2\text{X}_2\text{L}$ systems, and the corresponding Gibbs interaction energies were estimated, assuming that the BSSE corrections to vibration motions are negligible. The influence of electron correlation on structures and relative energies has been examined by full geometry optimizations using the density functional theory (DFT) with the B3LYP hybrid functional. Some tests at the correlated MP2 level have also been performed. Total energies are given in Table S1. The deformation energy ΔE_{def} of the ligand L upon complexation was estimated as the energy difference between the structures of L uncomplexed and of L within the complex, thus giving insights into the effect of geometry changes for the electronically relaxed ligand. Insights into the electron distribution are given by the analysis of Mulliken charges, which can be compared with previous results obtained with the same methodologies.^{22,23}

3. Results

We first discuss the ligand interactions with the “naked” uranyl ion ($\text{UO}_2\text{L}_n^{2+}$, $\text{UO}_2\text{L}_2^{2+}$, and $\text{UO}_2\text{L}_3^{2+}$ species with L

- (30) Frisch, M. J.; Trucks, G. W.; Schlegel, H. B.; Scuseria, G. E.; Robb, M. A.; Cheeseman, J. R.; Zakrzewski, V. G.; Montgomery, J. A., Jr.; Stratmann, R. E.; Burant, J. C.; Dapprich, S.; Millam, J. M.; Daniels, A. D.; Kudin, K. N.; Strain, M. C.; Farkas, O.; Tomasi, J.; Barone, V.; Cossi, M.; Cammi, R.; Mennucci, B.; Pomelli, C.; Adamo, C.; Clifford, S.; Ochterski, J.; Petersson, G. A.; Ayala, P. Y.; Cui, Q.; Morokuma, K.; Malick, D. K.; Rabuck, A. D.; Raghavachari, K.; Foresman, J. B.; Cioslowski, J.; Ortiz, J. V.; Stefanov, B. B.; Liu, G.; Liashenko, A.; Piskorz, R.; Komaromi, I.; Gomperts, R.; Martin, R. L.; Fox, D. J.; Keith, T.; Al-Laham, M. A.; Peng, C. Y.; Nanayakkara, A.; Gonzalez, C.; Challacombe, M.; Gill, P. M. W.; Johnson, B. G.; Chen, W.; Wong, M. W.; Andres, J. L.; Head-Gordon, M.; Replogle, E. S.; Pople, J. A. *Gaussian 98*, revision A.5; Gaussian, Inc.: Pittsburgh, PA, 1998.
- (31) Ortiz, J. V.; Hay, P. J.; Martin, R. L. *J. Am. Chem. Soc.* **1992**, *114*, 2736–2737 and references therein.
- (32) Hutschka, F.; Troxler, L.; Dedieu, A.; Wipff, G. *J. Phys. Chem. A* **1998**, *102*, 3773–3781.
- (33) Sémon, L.; Boehme, C.; Billard, I.; Hennig, C.; Lützenkirchen, K.; Reich, T.; Rossberg, A.; Rossini, I.; Wipff, G. *ChemPhysChem* **2001**, *2*, 591–598.
- (34) Küchle, W.; Dolg, M.; Stoll, H.; Preuss, H. *J. Chem. Phys.* **1994**, *100*, 7535–7542.
- (35) ECPs and corresponding valence basis sets from Institut für Theoretische Chemie, Universität Stuttgart, <http://www.theochem.uni-stuttgart.de> (2003).
- (36) Boys, S. F.; Bernardi, F. *Mol. Phys.* **1970**, *19*, 553–566.

bidentate). The effect of counterions is then considered in neutral $\text{UO}_2\text{X}_2\text{L}$ complexes, for which bidentate and monodentate AcA and AccA ligands are compared, with Cl^- versus NO_3^- as counterions. Unless otherwise indicated, all results correspond to HF calculations and BSSE corrected interaction energies ΔE with the large core ECPs on the U atom. The results obtained with other methodologies (DFT and MP2 calculations, and comparison of large core ECPs versus smaller core ECPs) are considered in the Discussion section of the paper.

The conformation of the ligands may be defined by C–C dihedral angles (ω_1 , ω_2 , ψ ; see Figure 1). For simplicity, we use the ϕ angle between the carbonyl dipoles which ranges from 0° for a *cis* ligand to 180° for the *trans* ligand and is thus a measure for the planarity of L. Changes in the O–U–O bite angle, often interpreted as indication of “strain” of the bound ligand, are also discussed. The main energy, structural, and electronic results are given in Tables 1–5 and Figures 2–6 and as Supporting Information.

3.1. Comparison of the $\text{UO}_2\text{L}_n^{2+}$, $\text{UO}_2\text{L}_2^{2+}$, and $\text{UO}_2\text{L}_3^{2+}$ Bidentate Complexes. The optimized AcA and AccA free ligands roughly adopt *trans* or *gauche* conformations of C_2 type symmetry, as a result of the dipole–dipole repulsions between the C=O groups: the dihedral angle ϕ is 167° and 119° , respectively. This is consistent with other calculations on AcA³⁷ and with the X-ray structure of the N–H analogue of AccA³⁸ and contrasts with the optimized $\text{UO}_2\text{L}_n^{2+}$ complexes ($n = 1–3$), in which the ligands are bidentate and *cis*. The only exception concerns the $\text{UO}_2(\text{AccA})_3^{2+}$ complex, for which no energy minimum could be located for the tris-bidentate form and one AccA oxygen lost its coordination to the U atom during the minimization process, while retaining a *gauche* conformation ($\phi = 70^\circ$). The main structural and energy results are given in Table 1 and Figure 2.

Intrinsically (i.e., in the absence of other competing species), AccA interacts better than AcA with the uranyl cation. This can be seen in the $\text{UO}_2\text{L}_n^{2+}$ complexes, where the preference $\Delta E_{6/7}$ for 7-chelate amounts to 7.8 kcal/mol. Adding a second ligand to form the $\text{UO}_2\text{L}_2^{2+}$ complexes is again more favorable for AccA (by 2 kcal/mol), as is the average per ligand interaction energy $\Delta E'$ (by 5.2 kcal/mol). The preference for AccA over AcA in the $\text{UO}_2\text{L}_n^{2+}$ and $\text{UO}_2\text{L}_2^{2+}$ complexes can be attributed to the larger electron transfer to uranyl (by 0.04 to 0.02 e, respectively) and stronger polarization of the O=C bonds, related to the “more linear” C=O–U angles (Figures S1 and S2). The $\text{UO}_2\text{L}_n^{2+}$ complexes adopt approximate 2-fold C_2 symmetry when $n = 1$ and have no perfect symmetry when $n = 2$ or 3. The U atom is quasiequidistant from the two carbonyl oxygens, and the U–L bond lengths are found to increase with n (by ≈ 0.12 Å from $n = 1$ to 2, and 0.19 Å from $n = 2$ to 3). Concomitantly, the U–O=C angles and the bite angle O–U–O decrease. Nonplanarity of the ligand also increases

(37) Sandrone, G.; Dixon, D. A.; Hay, B. P. *J. Phys. Chem.* **1999**, *103*, 3554–3561.

(38) Aleman, C.; Navarro, E.; Puiggali, J. *J. Org. Chem.* **1995**, *60*, 6135–6140.

Table 1. Main Structural Parameters (Distances in Å and Angles in deg) and BSSE Corrected Interaction Energies from HF Calculations (kcal/mol) for $\text{UO}_2\text{L}_n^{2+}$ Complexes^a

		$\langle\text{U}-\text{O}\rangle^b$	$\langle\text{O}=\text{C}\rangle^c$	$\text{U}=\text{O}^d$	β	$\langle\alpha\rangle^e$	ϕ	$\Delta E'$	ΔE	ΔE_{def}
AcA			1.206				167			
AccA			1.205				119			
UO_2^{2+}				1.651						
$[\text{UO}_2(\text{AcA})]^{2+}$	L ₁	2.280	1.262	1.685	72	143	0		-174.0	27.8
$[\text{UO}_2(\text{AccA})]^{2+}$	L ₁	2.270	1.271	1.688	81	147	26		-181.8	30.0
$[\text{UO}_2(\text{AcA})_2]^{2+}$	L ₁	2.391	1.242	1.704	69	142	9	-139.9	-105.0	20.8
	L ₂	2.406	1.245		70	138	20			19.9
$[\text{UO}_2(\text{AccA})_2]^{2+}$	L ₁	2.395	1.247	1.707	76	148	-24	-145.1	-107.0	19.4
	L ₂	2.393	1.247		77	148	22			19.6
$[\text{UO}_2(\text{AcA})_3]^{2+}$	L ₁	2.570	1.227	1.706	61	139	-42	-106.0	-23.8	14.7
	L ₂	2.549	1.227		62	139	-36			15.4
	L ₃	2.549	1.227		62	139	-36			15.4
$[\text{UO}_2(\text{AccA})_3]^{2+}$	L ₁	2.470	1.237		70	150	13	-107.5	-27.7	16.4
	L ₂	2.494	1.238		69	142	-37			16.8
	L ₃ ^f	3.688	1.227		29	135	-70			11.9

^a Distances are given in Å, and angles are given in deg. See eqs 1–3 for definitions. A full version is given as Supporting Information (Table S2).
^b Average of the U–O₁ and U–O₂ distances. ^c Average of the O₁=C₁ and O₂=C₂ distances. ^d The two axial U=O_A and U=O_B bond lengths are identical.
^e Average of the α_1 and α_2 angles. ^f This ligand becomes monodentate during the optimization, with U–O₁ = 2.408 Å and U–O₂ = 4.967 Å.

Table 2. BSSE Corrected Interaction Energies ΔE (kcal/mol) as Defined in Equations 1–3 for $\text{UO}_2\text{Cl}_2\text{L}$ and $\text{UO}_2(\text{NO}_3)_2\text{L}$ Bidentate and Monodentate Complexes^a

	L	UO_2X_2	bidentate				monodentate				
			ΔE	$\Delta E_{\text{NO}_3/\text{Cl}}$	$\Delta E_{6/7}$	ΔE_{def}	ΔE	$\Delta E_{\text{NO}_3/\text{Cl}}$	$\Delta E_{6/7}$	$\Delta E_{\text{mono/bi}}$	ΔE_{def}
HF//HF	AccA	UO_2Cl_2	-53.4	0.0	0.0	10.4	-43.4	0.0	0.0	10.0	4.0
	AcA	UO_2Cl_2	-47.5	0.0	5.9	13.1	-40.0	0.0	3.4	7.5	4.9
	AccA	$\text{UO}_2(\text{NO}_3)_2$	-41.0	12.4	0.0	10.4	-39.7	3.7	0.0	1.3	4.2
	AcA	$\text{UO}_2(\text{NO}_3)_2$	-38.2	9.3	2.8	13.3	-37.5	2.5	2.2	0.7	4.5
	AccA	$\text{UO}_2(\text{NO}_3)_2^b$	-40.6		0.0	10.4	-39.6		0.0	1.0	4.2
	AcA	$\text{UO}_2(\text{NO}_3)_2^b$	-37.6		3.0	13.6	-37.3		2.3	0.3	4.5
DFT//DFT	AccA	UO_2Cl_2	-45.7	0.0	0.0	7.0	-36.9	0.0	0.0	8.8	3.0
	AcA	UO_2Cl_2	-37.6	0.0	8.1	13.4	-31.6	0.0	5.3	6.0	6.3
	AccA	$\text{UO}_2(\text{NO}_3)_2$	-34.2	11.5	0.0	7.3	-32.3	4.6	0.0	1.9	3.4
	AcA	$\text{UO}_2(\text{NO}_3)_2$	-28.7	8.9	5.5	13.3	-27.1	4.5	5.2	1.6	6.2
	AccA	$\text{UO}_2(\text{NO}_3)_2^b$	-36.8		0.0	7.8	-35.0		0.0	1.8	3.5
	AcA	$\text{UO}_2(\text{NO}_3)_2^b$	-31.6		5.2	13.9	-30.0		5.0	1.6	6.5
MP2//DFT	AccA	UO_2Cl_2	-52.9	0.0	0.0	6.2	-40.6	0.0	0.0	12.3	1.9
	AcA	UO_2Cl_2	-43.0	0.0	9.9	13.5	-34.0	0.0	6.6	9.0	5.5
	AccA	$\text{UO}_2(\text{NO}_3)_2$	-44.2	8.7	0.0	6.3	-41.2	0.6	0.0	2.0	2.2
	AcA	$\text{UO}_2(\text{NO}_3)_2$	-36.3	6.7	7.9	13.6	-34.8	0.8	6.4	1.5	5.5

^a Differences between $\text{UO}_2\text{Cl}_2\text{L}$ and $\text{UO}_2(\text{NO}_3)_2\text{L}$ complexes ($\Delta E_{\text{NO}_3/\text{Cl}}$), between monodentate and bidentate complexes ($\Delta E_{\text{mono/bi}}$), and between AcA and AccA ligands ($\Delta E_{6/7}$). The corresponding Gibbs free energies are given in Table 4. Uncorrected interaction energies are given in Table S4. Unless otherwise indicated, the results are obtained with large ECPs on U. ^b Calculation with small core Stuttgart group's ECPs.

with n and is more pronounced with AccA than with AcA. The charge transfer Δq from the ligand(s) to the uranyl cation increases as expected with the number of ligands (from 0.4 e for $n=1$ to 0.6 e for $n=3$). Also note that the axial U=O distances increase with the number of coordinated ligands and are larger with AccA than with AcA, in keeping with the stronger interactions with the former ligand.

In the $\text{UO}_2\text{L}_3^{2+}$ complexes, the equatorial coordination number CN of uranyl is 6, which is common when bidentate anions (e.g., nitrates, carboxylates) sit in the equatorial plane,^{24,39,40} but leads to important strain and repulsions between the three ligands. Internal strain can be seen in the structure of $\text{UO}_2(\text{AcA})_3^{2+}$ in which the carbonyl oxygens markedly deviate from the equatorial plane (Figure S3). In the $\text{UO}_2(\text{AccA})_3^{2+}$ complex, these repulsions seem to be still stronger, as indicated by the loss of one U–O(L) bond during

the energy “minimization” process.⁴¹ Thus, evolution of the $\text{UO}_2(\text{AccA})_3^{2+}$ complex from a 6 to 5 equatorial coordination is indicative of stronger steric demand with the AccA bidentate ligand.⁴²

3.2. $\text{UO}_2\text{Cl}_2\text{L}$ and $\text{UO}_2(\text{NO}_3)_2\text{L}$ Bidentate Complexes: The Influence of Counterions. The bidentate $\text{UO}_2\text{X}_2\text{L}$ complexes adopted a quasi-2-fold symmetry, in which the U atom is equatorially coordinated to the two anions and the ligand L, and equidistant from the two carbonyl oxygens. As L formally interacts with a neutral UO_2X_2 moiety, its binding energy is strongly reduced (by more than 120 kcal/mol), compared to that of the UO_2L^{2+} complexes. Again, the bidentate AccA ligand is preferred over AcA, with marked counterion effects on the corresponding $\Delta E_{6/7}$ energy

(41) No minimum could be found for this form, which might be less stable than the one with two *cis* bidentate + one *trans* (or *gauche*) monodentate AccA ligands.

(42) The bigger size of AccA, compared to AcA, can be seen for instance in the UO_2L^{2+} and $\text{UO}_2\text{L}_2^{2+}$ complexes in which the O···O intraligand distances are 0.25 Å longer with AccA than with AcA, while the interligand O···O distances are 0.2 Å shorter with AccA.

(39) Casellato, U.; Vigato, P. A.; Vidali, M. *Coord. Chem.* **1981**, *36*, 183–265.

(40) Leciejewicz, J.; Alcock, N.; Kemp, T. *Struct. Bonding* **1995**, *82*, 43–84.

Table 3. Main Structural Parameters and HF Results for $\text{UO}_2\text{X}_2\text{L}$ Complexes

L	UO_2X_2		U—O ₁	U—O ₂	O ₁ —C ₁	O ₂ —C ₂	U=O _A	U=O _B	$\langle\text{U}-\text{X}_1\rangle^{d,e}$	$\langle\text{U}-\text{X}_2\rangle^{d,e}$	β	α_1	α_2	δ	ϕ
AcA					1.206	1.206									167
AccA					1.205	1.205									119
	UO_2Cl_2						1.695	1.695	2.628	2.628				122	
AcA	UO_2Cl_2	bi	2.509	2.511	1.225	1.224	1.706	1.708	2.708	2.713	65	130	136	118	50
AcA	UO_2Cl_2	mono	2.393	4.774	1.243	1.206	1.700	1.701	2.685	2.711		148		137	95
AccA	UO_2Cl_2	bi	2.499	2.499	1.234	1.234	1.709	1.709	2.715	2.715	68	127	127	115	77
AccA	UO_2Cl_2	mono	2.359	4.687	1.246	1.212	1.700	1.702	2.694	2.711		159		141	-121
	$\text{UO}_2(\text{NO}_3)_2$						1.698	1.698	2.463	2.463				180	
AcA	$\text{UO}_2(\text{NO}_3)_2$	bi	2.546	2.546	1.221	1.221	1.711	1.711	2.535	2.535	62	137	137	118	45
AcA	$\text{UO}_2(\text{NO}_3)_2$	mono	2.394	4.690	1.239	1.206	1.705	1.707	2.499	2.522		154		146	92
AccA	$\text{UO}_2(\text{NO}_3)_2$	bi	2.554	2.554	1.230	1.230	1.712	1.712	2.533	2.533	64	129	129	115	75
AccA	$\text{UO}_2(\text{NO}_3)_2$	mono	2.389	4.664	1.245	1.212	1.707	1.707	2.503	2.519		158		141	-116
							SCRF								
AcA	$\text{UO}_2(\text{NO}_3)_2$	bi	2.478	2.477	1.228	1.228	1.711	1.711	2.571	2.571	64	144	144	112	19
AccA	$\text{UO}_2(\text{NO}_3)_2$	bi	2.491	2.491	1.236	1.236	1.711	1.711	2.577	2.577	67	137	137	110	59
							X-ray								
AcA	$\text{UO}_2(\text{NO}_3)_2$	bi ^b	2.409	2.409	1.171	1.171	1.775	1.775	2.513	2.513	66	139	139	112	36
AccA	$\text{UO}_2(\text{NO}_3)_2$	bi ^c	2.323	2.392	1.228	1.262	1.750	1.734	2.535	2.539	71	135	136	108	61

^a Distances are given in Å, and angles are given in deg. A full version is given as Supporting Information (Table S5). ^b Refcode: XEVNAN. ^c Refcode: HEPGEO in the CSD. ^d X = Cl in chloro complexes or O in nitrate complexes. ^e Average of the U—O_{NO₃} distances.

Table 4. BSSE Corrected Gibbs Free Energies from HF Calculations (kcal/mol) for UO_2^{2+} , $\text{UO}_2\text{Cl}_2\text{L}$, and $\text{UO}_2(\text{NO}_3)_2\text{L}$ Bidentate and Monodentate Complexes^a

L	UO_2X_2	bidentate			monodentate			
		ΔG°	$\Delta G^\circ_{\text{NO}_3/\text{Cl}}$	$\Delta G^\circ_{6/7}$	ΔG°	$\Delta G^\circ_{\text{NO}_3/\text{Cl}}$	$\Delta G^\circ_{6/7}$	$\Delta G^\circ_{\text{mono/bi}}$
AccA	UO_2^{2+}	-169.4		0.0				
AcA	UO_2^{2+}	-162.5		6.9				
AccA	UO_2Cl_2	-38.0	0.0	0.0	-30.2	0.0	0.0	7.8
AcA	UO_2Cl_2	-35.2	0.0	2.8	-28.1	0.0	2.1	7.1
AccA	$\text{UO}_2(\text{NO}_3)_2$	-24.7	13.3	0.0	-24.5	5.7	0.0	0.2
AcA	$\text{UO}_2(\text{NO}_3)_2$	-24.4	10.8	0.3	-24.4	3.7	0.1	0.0

^a The differences in ΔG° values ($\Delta G^\circ_{\text{NO}_3/\text{Cl}}$, $\Delta G^\circ_{6/7}$, $\Delta G^\circ_{\text{mono/bi}}$) are defined in Table 2. Uncorrected energies are given in Tables S9 and S10

difference: it is larger with Cl^- than with NO_3^- counterions (by 5.9 vs 2.8 kcal/mol, respectively). The main results are given in Tables 2 (energies), 3 (structural characteristics), and S6 (Mulliken charges).

Let us first discuss the $\text{UO}_2\text{Cl}_2\text{L}$ complexes with chloride counterions. Their optimized structures (see Figure 3 and Table 3) indeed show a lengthening of the U—L bonds (by about 0.3 Å), compared to the corresponding UO_2L^{2+} complexes. The lowered cation charge ($q_{\text{UO}_2} \approx 1.0$ e; see Table S6) leads to fewer charge—dipole interactions, and diminished $\text{O}^{\delta-}\text{C}^{\delta+}$ polarization of the carbonyl bonds, thus weakening the uranyl—L interaction. The greater U—L bond lengths engender further changes, like the decrease in the O—U—O bite angle, the reduction of the C=O—U angles, and the enlargement of the dihedral angle ϕ with the two ligands. None of the $\text{UO}_2\text{X}_2\text{L}$ complexes are planar, and the nonplanarity is more pronounced with a 7-chelate than with a 6-chelate ring ($\phi = 77^\circ$ and 50° , respectively). As expected, the AcA and AccA ligands are less strained in $\text{UO}_2\text{Cl}_2\text{L}$ than in UO_2L^{2+} complexes, as indicated by their deformation energies ΔE_{def} which are about 20 kcal/mol smaller. Again, ΔE_{def} is smaller for the 7-chelating ligand than for the 6-chelating ligand (by ≈ 3 kcal/mol).

All of the described trends for the bidentate $\text{UO}_2\text{Cl}_2\text{L}$ complexes are also observed for the $\text{UO}_2(\text{NO}_3)_2\text{L}$ complexes with nitrates as counterions (see Table 3 and Figure 3). In the latter, nitrates are also bidentate, leading to a CN of 6. The corresponding ligand binding energies ΔE are clearly

smaller than in the $\text{UO}_2\text{Cl}_2\text{L}$ complexes (by $\approx 12-9$ kcal/mol), which correspond to somewhat longer U—L bonds ($\Delta \approx 0.05$ Å), less elongated C=O bonds ($\Delta \approx 0.01$ Å), and a reduced bite angle ($\Delta \approx 3^\circ$). There is also less electron transfer to uranyl with nitrate than with chloride counterions ($\Delta \approx 0.3$ e), due to the harder character and lower electron donating capability of the nitrate ions. The ligand deformation energies are similar to those in chloro complexes.

3.3. $\text{UO}_2\text{Cl}_2\text{L}$ and $\text{UO}_2(\text{NO}_3)_2\text{L}$ Monodentate Complexes. Comparison with Bidentate Analogues. Upon optimization of the complexes with AcA or AccA monodentate, the ligands retained a monodentate coordination and *gauche* type conformations ($\phi = 95^\circ$ and 121° , respectively).⁴³ The main structural results are given in Table 3 and Figure 4. The U—L bond distances for the complexed binding site shorten considerably (by more than 0.10 Å), compared to the bidentate form, while the U=O bond lengthens (by ≈ 0.005 Å) which indicates an enhanced interaction compensating for the lost second bond. They are again somewhat longer with NO_3^- than with Cl^- counterions (by ≈ 0.03 Å), and longer with AccA than AcA as ligand ($\Delta \approx 0.03$ Å in $\text{UO}_2\text{Cl}_2\text{L}$ complexes and 0.005 Å in $\text{UO}_2(\text{NO}_3)_2\text{L}$ complexes), thus indicating stronger interactions of L with the chloride salt and, for the latter, a preference for AccA over AcA. This is confirmed by the binding

(43) Optimization of the $\text{UO}_2(\text{NO}_3)_2(\text{AccA})$ complex starting with a *trans* ligand led to another energy minimum at $\phi = 180^\circ$, which turned out to be 3 kcal/mol less stable than with AccA *gauche* ($\phi = 120^\circ$).

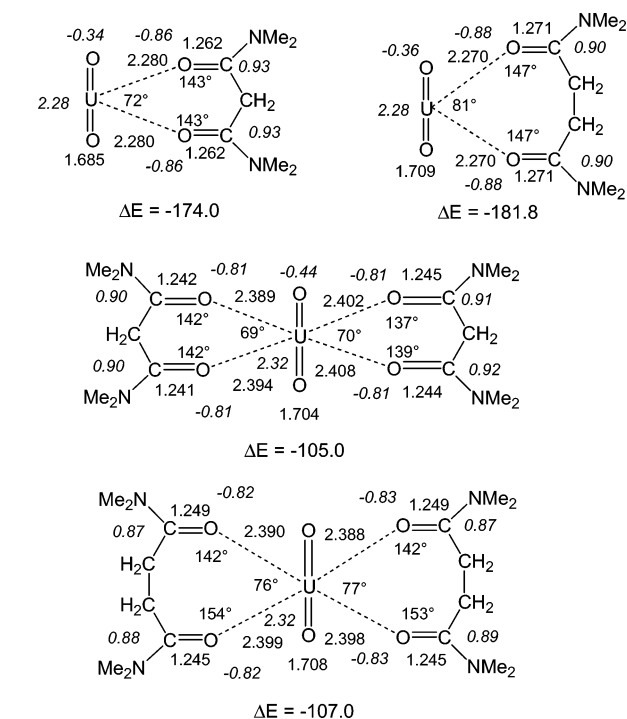


Figure 2. HF optimized UO_2L^{2+} and $\text{UO}_2\text{L}_2^{2+}$ bidentate complexes (L = AcA vs AccA), with selected distances (Å) and angles (deg), interaction energies ΔE (kcal/mol), and Mulliken charges (in italics).

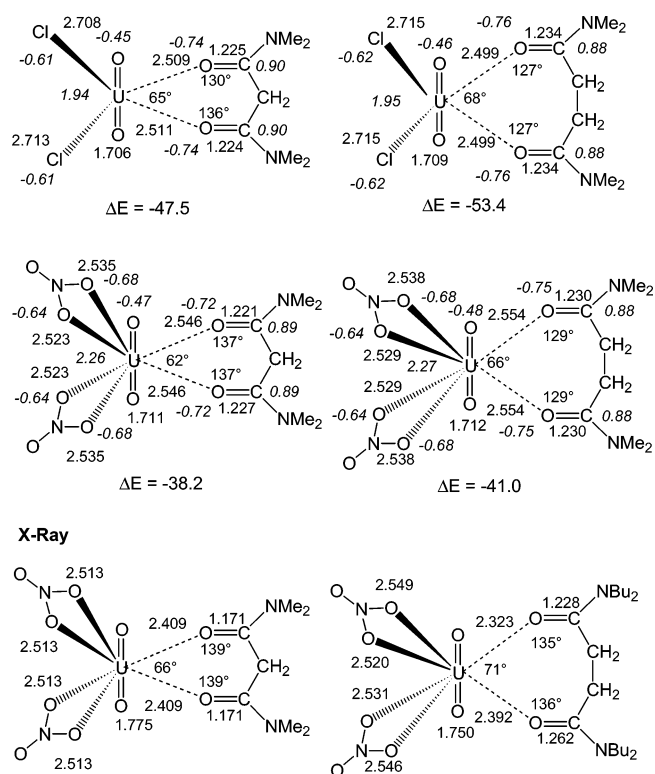


Figure 3. HF optimized $\text{UO}_2\text{Cl}_2\text{L}$ and $\text{UO}_2(\text{NO}_3)_2\text{L}$ bidentate complexes (L = AcA vs AccA), with selected distances (Å) and angles (deg), interaction energies ΔE (kcal/mol), and Mulliken charges (in italics).

energies ΔE which are 3–4 kcal/mol weaker with nitrate than with chloride counterions and, for a given anion, 2–3 kcal/mol larger with AccA than with AcA. There is thus some ligand size effect on monodentate coordination, presumably due to secondary interactions beyond the coord-

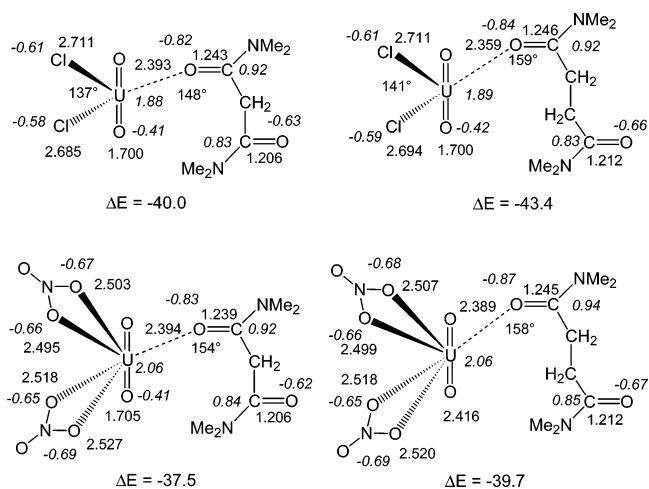


Figure 4. $\text{UO}_2\text{Cl}_2\text{L}$ and $\text{UO}_2(\text{NO}_3)_2\text{L}$ monodentate complexes (L = AcA vs AccA), with selected distances (Å) and angles (deg), interaction energies ΔE (kcal/mol), and Mulliken charges (in italics) (HF optimizations).

inated centers. The ligand deformation energies ΔE_{def} , similar for AccA and AcA (see Table 2), are, as expected, smaller (by 6–8 kcal/mol) than in the bidentate complexes.

Turning now to the comparison of the mono- versus bidentate coordination of a given ligand, it can be seen that the corresponding energy difference $\Delta E_{\text{mono/bi}}$ is positive (i.e., chelating coordination is preferred) and ranges from 10.0 kcal/mol (for the $\text{UO}_2\text{Cl}_2\text{AccA}$ complex) to 0.7 kcal/mol (for $\text{UO}_2(\text{NO}_3)_2\text{AcA}$). Thus, $\Delta E_{\text{mono/bi}}$ is smaller for the nitrate complexes (0.7 and 1.3 kcal/mol) than for the chloro complexes (7.5 and 10.0 kcal/mol), and smaller with the 7-chelating ligand than with the 6-chelating ligand (by 2.5 kcal/mol in the chloro complexes and 0.6 kcal/mol in the nitrate complexes). Although $\Delta E_{\text{mono/bi}}$ energies depend on the interplay of many contributions (uranyl–L attractions, avoided repulsions in the coordination sphere, and deformation energies of L), one can notice that they follow the same trends as the ligand binding energies ΔE , as far as the anion effect and chelate ring size effect are concerned.

The reported $\Delta E_{\text{mono/bi}}$ energy differences correspond to energy minima of the monodentate versus bidentate forms. However, as the monodentate ligand is somewhat less constrained and more flexible than the bidentate ligand, its vibration spectrum should be richer in low frequency motions, which lead to further stabilization. We thus calculated the corresponding Gibbs free energies at 300 K. The results (Table 4) indeed show a decrease of $\Delta G_{\text{mono/bi}}^\circ$, compared to $\Delta E_{\text{mono/bi}}$ (by about 0.4–2.5 kcal/mol; the largest contribution is found for the weakest complex, as anticipated). Thus, in the case of the nitrate complexes, the monodentate and bidentate coordinations of L have quasisimilar stabilities ($\Delta G_{\text{mono/bi}}^\circ = 0.0$ and 0.2 kcal/mol for AcA and AccA, respectively), while for the chloro complexes, the preference for bidentate coordination remains significant (7.1 and 7.8 kcal/mol, respectively). The changes in Gibbs energies confirm the higher stability of the 7-ring compared to the 6-ring chelate with the chloro complexes, while with the nitrate complexes, this preference almost vanishes ($\Delta G_{67}^\circ = 0.1$ kcal/mol).

Table 5. Energies (kcal/mol) of the Isodesmic Reaction Defined in Figure 5^a

L	UO ₂ X ₂		HF//HF			DFT//DFT			MP2//DFT		
			ΔE_{iso}	$\Delta E_{\text{NO}_3/\text{Cl}}$	$\Delta E_{6/7}$	ΔE_{iso}	$\Delta E_{\text{NO}_3/\text{Cl}}$	$\Delta E_{6/7}$	ΔE_{iso}	$\Delta E_{\text{NO}_3/\text{Cl}}$	$\Delta E_{6/7}$
AccA	UO ₂ Cl ₂	<i>trans</i>	-16.5	0.0	6.4	-15.9	0.0	8.4	-14.8	0.0	11.5
AcA	UO ₂ Cl ₂	<i>trans</i>	-22.9	0.0	0.0	-24.3	0.0	0.0	-26.3	0.0	0.0
AccA	UO ₂ (NO ₃) ₂	<i>trans</i>	-13.9	2.6	3.7	-11.9	4.0	6.5			
AcA	UO ₂ (NO ₃) ₂	<i>trans</i>	-17.6	5.3	0.0	-18.4	5.9	0.0			0.0
AccA	UO ₂ Cl ₂	<i>cis</i>	-12.6	0.0	6.4						
AcA	UO ₂ Cl ₂	<i>cis</i>	-19.0	0.0	0.0						
AccA	UO ₂ (NO ₃) ₂	<i>cis</i>	-12.5	0.1	3.7						
AcA	UO ₂ (NO ₃) ₂	<i>cis</i>	-16.2	2.8	0.0						

^a See Table 2 for definitions.

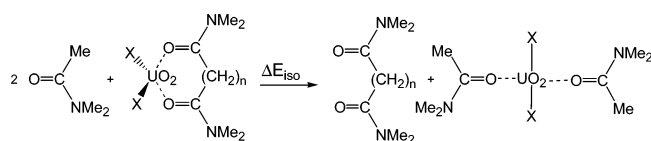


Figure 5. Isodesmic reaction for changing one bidentate ligand L into two monoamide analogues ($X^- = \text{Cl}^-$ or NO_3^-).

3.4. Isodesmic Reactions Exchanging One Bidentate Ligand to Two Monodentate Analogues. In the preceding subsection, we compared the bidentate versus monodentate binding modes of a given bifunctional ligand, which corresponds to a change in uranyl coordination number CN from 6 to 5 with nitrate anions and 4 to 3 with chloride anions. In order to gain further insights into the chelate effect, we also considered the exchange of a bidentate ligand with two monodentate amide A analogues (see Figure 5), thus retaining a constant CN. The energies ΔE_{iso} of the corresponding isodesmic reactions have been calculated as a function of the anion of the ligand (see Table 5). We notice that in the UO₂X₂(A)₂ complexes the two A monoamide ligands prefer to be *trans* instead of *cis*, thus minimizing their mutual repulsions, as well as the X⁻/X⁻ repulsions. A *trans* arrangement is indeed observed in solid state structures of UO₂(NO₃)₂(monoamide)₂ complexes⁴⁴ and their analogues,³⁹ in the optimized UO₂(NO₃)₂(H₂O)₂ complex,⁴⁵ and further supported by energy comparison of the two forms ($\Delta E_{\text{cis/trans}} = 1.4$ and 3.9 kcal/mol, respectively, for nitrate and chloro complexes; HF optimizations).

For the two ligands and two anions considered, the energies ΔE_{iso} of the isodesmic reactions are clearly negative; i.e., two monodentate ligands are preferred (by 16.5–22.9 kcal/mol with Cl⁻ and 13.9–17.6 kcal/mol with NO₃⁻ counterions). Furthermore, the reaction is more exothermic with Cl⁻ than with NO₃⁻ counterions (by 5.3 kcal/mol with AcA and 2.6 kcal/mol with AccA). For a given anion, it is also more exothermic with 6-ring than with 7-ring forming ligands (by 6.4 kcal/mol with Cl⁻ anions and 3.7 kcal/mol with NO₃⁻).

4. Discussion and Conclusions

Quantum mechanical investigations reveal important structural, electronic, and energetic aspects of the coordination

of di-oxygen ligands to the uranyl cation in the gas phase and allow us to directly compare the two binding modes of a given bifunctional ligand, as well as a bidentate ligand to two monofunctional analogues. Among the studied complexes, UO₂(NO₃)₂L can be considered as the most “realistic” ones, as they are derived from solid state structures and correspond to a saturated first coordination sphere of uranium. Whether the UO₂Cl₂L chloro complexes are saturated or not remains to be assessed, but the corresponding CN of 4, although observed in solid state structures, is quite low.⁴⁶ As concerns the charged complexes, UO₂L²⁺ and UO₂L₂²⁺ are unsaturated, while UO₂L₃²⁺ complexes are saturated. According to our calculations, the preference for 6- versus 7-chelates and for bi- versus monodentate complexation indeed depends on the degree of saturation and “strain” in the first coordination sphere. Thus, in the UO₂L²⁺, UO₂L₂²⁺, and UO₂Cl₂L complexes, the formation of a 7-ring chelate is favored over a 6-ring chelate, and bidentate coordination is clearly preferred. This contrasts with the saturated UO₂(NO₃)₂L complexes, in which the energy difference between 6- and 7-chelating ligands, as well as the energy difference between a given mono- and bidentate coordinated ligand, almost vanishes. There is thus a marked counterion effect on the preferred chelate size and on mono- versus bidentate coordination mode. These results concern gas phase complexation, for which no experimental data are available.

In the following, we first address some computational issues. This is followed by a discussion on the preference for bi- versus monodentate coordination and for 6- versus 7-membered ring chelate in the gas phase for the diamide ligands. We also address the question of further stabilization of the monodentate ligation in the presence of other coordinating oxygen species and compare bidentate diamide versus bis-monoamide ligands.

4.1. Computational Issues: The Effect of Electron Correlation and of ECPs. The results presented in the preceding sections are based on BSSE corrected HF energies and thus do not include correlation effects. We decided to investigate the effect of electron correlation by optimizing all UO₂L²⁺ and UO₂X₂L complexes at the DFT level of theory, as well as performing single point MP2 calculations on selected DFT optimized structures. As found in previous studies,^{22,47,48} the conclusions derived at the HF level were

(44) Clement, O.; Rapko, B. M.; Hay, B. P. *Coord. Chem. Rev.* **1998**, *170*, 203–243.

(45) Craw, J. S.; Vincent, M. A.; Hillier, I. H.; Wallwork, A. L. *J. Phys. Chem.* **1995**, *99*, 10181–10185.

(46) In the Cambridge Crystallographic Structural Database, 18 structures contain the UO₂Cl₂ unit plus either 2 oxygens (from ketones, urea, phosphin oxide, phosphoramidate) or 3 oxygens (with small ligands such as H₂O, formamide, THF) in the equatorial plane.

confirmed by these calculations (Tables 2 and 5). When compared to the HF energies, one notes that DFT leads to an increase of the uranyl–L interaction in UO_2L^{2+} complexes (by ~ 20 kcal/mol) and to a decrease in the $\text{UO}_2\text{Cl}_2\text{L}$ and $\text{UO}_2(\text{NO}_3)_2\text{L}$ complexes (by ~ 8 kcal/mol). All trends discussed here are the same, however, on both DFT and HF levels. (i) Most notably, in all systems, AccA is preferred over AcA. The corresponding $\Delta E_{6/7}$ energy difference is about 2 kcal/mol larger at the DFT than at the HF level. (ii) The two studied ligands bind more strongly to the chloro than to the nitrate complexes, and the anion effect is about 3 kcal/mol stronger with AccA than with AcA. (iii) The energy difference $\Delta E_{\text{mono/bi}}$ between mono- and bidentate coordination follows the same order. It is largest in the chloro complex with AccA (~ 9 kcal/mol) and smallest in the nitrate complex with AcA (~ 2 kcal/mol). In $\text{UO}_2\text{X}_2\text{L}$ complexes, $\Delta E_{\text{mono/bi}}$ is also larger with AccA than with AcA (by ~ 3 kcal/mol when $\text{X}^- = \text{Cl}^-$ and 0.3 kcal/mol when $\text{X}^- = \text{NO}_3^-$). For both ligands, the $\Delta E_{\text{mono/bi}}$ difference is small (< 2 kcal/mol) in the nitrate complexes. (iv) The energies of the isodesmic reactions exchanging a bidentate ligand to two monodentate analogues are within a few kilocalories per mole the same and confirm the preference for bis-monodentate over bidentate coordination (Table 5). (v) The deformation energies of the ligand upon complexation are similar and follow the same trends at both levels of theory. Energies obtained at the MP2 level of theory also yield to similar conclusions (see Tables 2 and 5).

Looking now at the effect of electron correlation on structural features, one sees that the optimized HF and DFT structures are similar (see Tables 3 and S7) and follow the same trends as far as the effect of anion (Cl^- vs NO_3^-), ligand (AccA vs AcA), and ligand binding mode (mono- vs bidentate) are concerned. The U–L bonds are somewhat shorter at the DFT level than at the HF level (by ~ 0.01 – 0.02 Å in the $\text{UO}_2\text{X}_2\text{L}$ complexes and 0.04 Å in UO_2L^{2+} complexes), as are the U–X bonds (by ~ 0.01 – 0.04 Å), while the axial U=O bonds are ~ 0.07 Å longer at the DFT level. Strictly speaking, these structures cannot be directly compared with those observed in the solid state, due to packing, dynamics, and environment effects. In the gas phase, cation–anion interactions are magnified, and hence, cation–ligand interactions are reduced, compared to a polar condensed phase. The effect of the surrounding dielectric medium can be illustrated by HF optimizations of the $\text{UO}_2(\text{NO}_3)_2\text{L}$ complexes using the SCRf solvation model implemented in Gaussian 98.³⁰ They indeed show (Table 3) that, compared to the “gas phase”, the U–O_{NO₃} bonds lengthen (by 0.04 Å) while the U–L bonds shorten (by ~ 0.06 – 0.07 Å). These distances come thus closer to those observed in the solid state but are still 0.05–0.07 Å longer.⁴⁹

Similar trends have been observed in previous calculations on lanthanide or uranyl complexes.^{33,48,50} Whether higher levels of calculations (e.g., CASSCF/CASPT2)⁵¹ would lead to better agreement with X-ray distances remains to be assessed, but such methods are presently too computer demanding for the studied systems.

Another issue concerns the representation of core electrons by effective core potentials. Because of computer limitations, we used “large” ECPs with 78 e in the core for all results discussed so far. Some of the calculations were, however, repeated using ECPs with a smaller core of 60 e, focusing on the $\text{UO}_2\text{X}_2\text{L}$ complexes. The results of HF and DFT optimization of $\text{UO}_2(\text{NO}_3)_2\text{L}$ complexes with small ECPs lead to similar energy differences as larger ECPs when one compares AcA versus AccA, and monodentate versus bidentate complexation (Table 2). The structures of these complexes are comparable to those obtained with the large ECPs (Table S5). When one moves from large to small core ECPs, the U–OL and U–O_{NO₂} distances somewhat shorten (the largest differences are ≈ 0.02 Å at both HF and DFT levels), but this is small, compared to the difference between calculated and X-ray structures, or between the two X-ray structures. Trends in the optimized parameters when one compares AcA versus AccA and monodentate versus bidentate coordination are also similar with the two ECPs (Table S5).

Another issue concerns the choice of relevant structures, as our optimizations started from solid state structures. Conformational sampling cannot be presently addressed by QM calculations alone, due to computer limitations. In the case of AccA uncomplexed, 22 conformers have been identified, whose relative energies somewhat depend on the level of theory.⁵² We notice, however, that the conformational freedom of the complexed ligands is quite limited and that if the selected structures would not correspond to the absolute minima, they are, at least, reasonable. Our main conclusions are thus unlikely to be altered by the multiple minima issue.

4.2. On the Preference for Bidentate versus Monodentate Coordination of a Given Diamide Ligand. Importance of Steric Strain. According to our calculations, the $\Delta E_{\text{mono/bi}}$ energy difference between mono- and bidentate binding modes of a given ligand depends on the anions and equatorial coordination number CN. In the absence of anions, structural evolutions from $\text{UO}_2\text{L}_2^{2+}$ to $\text{UO}_2\text{L}_3^{2+}$ bidentate complexes clearly indicate that the limit of strain has been reached with three ligands, especially with AccA ligands, for which the CN of 6 cannot be maintained. As far as the anion effect is concerned, anion X^- coordination to the UO_2L^{2+} complex not only weakens the U–L bonds but also leads to X/L and X/X repulsions which are larger with nitrate than with chloride anions. Oxygen atoms are less bulky than chloride anions, but nitrates are more space demanding in the equatorial plane than are chlorides, because they are

(47) Boehme, C.; Wipff, G. *J. Phys. Chem. A* **1999**, *103*, 6023–6029.

(48) Boehme, C.; Wipff, G. *Inorg. Chem.* **1999**, *38*, 5734–5741.

(49) Differences between calculated and X-ray structures should not be overinterpreted, as there are irregularities in X-ray structures as well. For instance, in the X-ray structure of the $\text{UO}_2(\text{NO}_3)_2(\text{AccA})$ complex the two U–OC bonds differ by 0.06 Å, while the two C=O bonds differ by 0.03 Å and are 0.06–0.09 Å longer than in the corresponding AcA complex (see refs 26 and 27).

(50) Spencer, S.; Gagliardi, K.; Handy, N. C.; Ioannou, A. G.; Skylaris, C.-K.; Willetts, A.; Simper, A. M. *J. Phys. Chem. A* **1999**, *103*, 1831–1837.

(51) Gagliardi, K.; Grenthe, I.; Roos, B. *Inorg. Chem.* **2001**, *40*, 2976–2978.

(52) Vargas, R.; Garza, J.; Dixon, D. A.; Hay, B. P. *J. Phys. Chem. A* **2002**, *104*, 5115–5121.

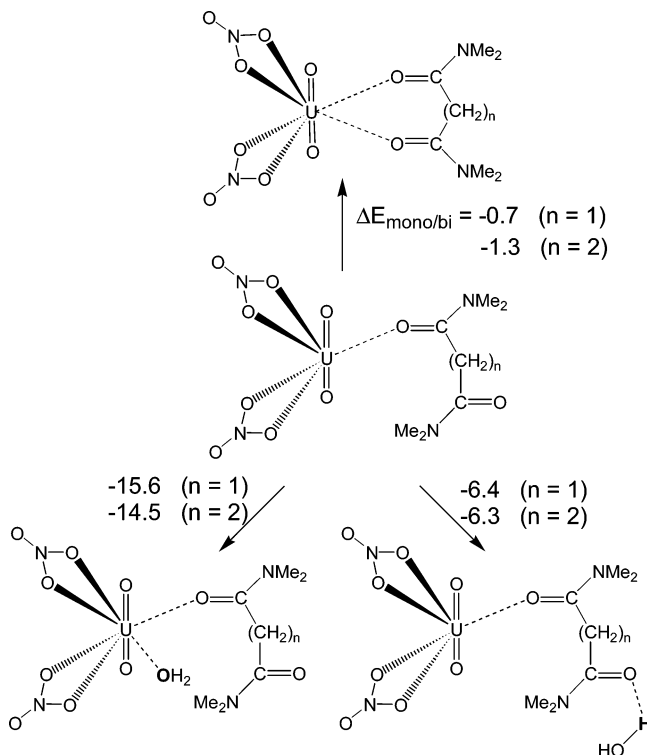


Figure 6. Energy stabilization (kcal/mol) for monodentate vs bidentate $\text{UO}_2(\text{NO}_3)_2\text{L}$ complexes and upon addition of one H_2O molecule to the monodentate form (HF optimizations + BSSE corrections).

bidentate, leading to a CN of 6 in the $\text{UO}_2(\text{NO}_3)_2\text{L}_{\text{bidentate}}$ complex. We notice that such a CN is commonly observed with two bidentate nitrate anions,^{24,53} while all-neutral oxygen ligands or larger anions (e.g. carboxylate⁴⁰) most often lead to a CN of 5 (as in the $\text{UO}_2(\text{H}_2\text{O})_5^{2+}$ “complex”).^{50,54} Thus, $\text{UO}_2(\text{NO}_3)_2\text{L}_{\text{bidentate}}$ complexes suffer important strain which is relieved when L becomes monodentate. Here, we find that the corresponding $\Delta E_{\text{mono/bi}}$ energy difference between energy minimized structures is very small (<2 kcal/mol at both DFT and HF levels of calculations), and that this number is further reduced by 1–2 kcal/mol when the contribution of vibrations to the Gibbs free energies are taken into account.

Not considered in these calculations is the $T\Delta S$ entropy cost for freezing the conformational freedom of the ligand when it moves from mono- to bidentate. An estimation of about 1 kcal/mol per rotatable bond can be found in the literature.⁵⁵ Subtracting thus another 1–2 kcal/mol (1–2 “free rotations” in L) would shift the preference toward monodentate, instead of bidentate, coordination of L in the $\text{UO}_2(\text{NO}_3)_2\text{L}$ complexes. In the less strained $\text{UO}_2\text{Cl}_2\text{L}$ complexes, such a correction should not be sufficient to reverse the preference for bidentate coordination. Thus, steric effects seem to be a key factor for chelating coordination. This concept is widely used in metal coordination chemistry (see, e.g., ref 56) and generally refers to the “size of atoms”,

as modeled by van der Waals type potentials in force field methods.^{57–60} Nonbonded atoms that are too close repulse each other. We note, however, that the “effective size” of atoms is not the same in the free and complexed ligand (due to perturbation of the electron cloud by orbital interactions, charge transfer, and polarization effects) and that “steric interactions” involve electrostatic interactions within the coordination sphere as well.⁶¹

Effect of Additional Ligands or Solvent Molecules. While the preceding discussion dealt with the simulated complexes, it can be worthwhile to speculate on perturbations brought about by additional coordinating species. Indeed, in condensed phases or in humid media, two other effects should further enthalpically favor monodentate coordination. First, the freed space left by unbound amide carbonyl may be occupied by another ligand. Second, the freed carbonyl oxygen may enjoy second shell stabilizing interactions, via, e.g., hydrogen bonding. In order to evaluate the corresponding energy stabilization ΔE , we partially optimized two forms of the $\text{UO}_2(\text{NO}_3)_2(\text{H}_2\text{O})\text{L}_{\text{monodentate}}$ complex, in which the added H_2O molecule is either coordinated to the U atom or hydrogen bonded to the “free” carbonyl oxygen. The results obtained for the AcA and AccA ligands (see Figure 6) indicate ΔE values of 15.6 and 14.5 kcal/mol, respectively, for U–OH₂ coordination, and of 6.4 and 6.3 kcal/mol, respectively, for C=O···HOH interactions. These are much larger than the $\Delta E_{\text{mono/bi}}$ or $\Delta G_{\text{mono/bi}}^\circ$ energy difference already reported, thus clearly shifting the enthalpic preference toward monodentate coordination.⁶² In the chloro $\text{UO}_2\text{X}_2(\text{H}_2\text{O})\text{L}_{\text{monodentate}}$ complexes, the enthalpic gain upon addition of an equatorial water molecule should be comparable as in nitrate complexes (or even larger, due to smaller steric crowding) and thus overcompensate for the $\Delta E_{\text{mono/bi}}$ preference (7–12 kcal/mol) for $\text{L}_{\text{bidentate}}$. As the structure of $\text{UO}_2\text{X}_2\text{L}_{\text{bidentate}}$ complexes prevents such stabilizing interactions, one must conclude that there is no enthalpic preference for bidentate complexation and that the latter, if observed, is due other effects, namely environment and entropic effects.

Binding Mode and Coordination Number. We notice that the comparison of the two binding modes of a given ligand also basically deals with the understanding of what

(53) Bombieri, G.; Paoli, G. D. In *Handbook on the Physics and Chemistry of Actinides*; Freeam, A. J., Keller, C., Eds.; Elsevier: Amsterdam, 1985; p 75.
 (54) Guilbaud, P.; Wipff, G. *J. Phys. Chem.* **1993**, *97*, 5685–5692 and references cited therein.
 (55) Searle, M. S.; Williams, D. H.; Gerhard, U. *J. Am. Chem. Soc.* **1992**, *114*, 10697–10704 and references therein.

(56) White, D.; Coville, N. J. *Adv. Organomet. Chem.* **1994**, *36*, 95–160.
 (57) Comba, P.; Gloe, K.; Inoue, K.; Krüger, T.; Stephan, H.; Yoshizuka, K. *Inorg. Chem.* **1998**, *37*, 3310–3315.
 (58) McDougall, G. J.; Hancock, R. D.; Boeyens, J. C. A. *J. Chem. Soc., Dalton Trans.* **1978**, 1438.
 (59) Hancock, R. D. *Acc. Chem. Res.* **1990**, *23*, 253–257.
 (60) Hay, B. P.; Clement, O.; Sandrone, G.; Dixon, D. A. *Inorg. Chem.* **1998**, *37*, 5887–5894.
 (61) To illustrate that point, we calculated the Coulombic interactions between the Mulliken atomic charges in the $\text{UO}_2\text{X}_2\text{L}$ monodentate and bidentate complexes. Despite the arbitrary definition of charges, the results (Table S12) indeed show that L is repulsed by the two anions, and ~10 kcal/mol more strongly by NO_3^- than by Cl^- anions. Nitrate anions also repulse each other more than chloride ligands do, and these repulsions are stronger in the bidentate complexes than in the monodentate complexes. One can also note that $\text{L}/\text{UO}_2\text{X}_2$ coulombic interactions are attractive and stronger with $\text{L}_{\text{bidentate}}$ than with $\text{L}_{\text{monodentate}}$, and stronger with AccA than with AcA ligands, in keeping with the other trends in the QM results.
 (62) Concerning the U–OH₂ interaction, we notice that the difference in ΔE values (~2 kcal/mol) with AccA ligand vs AcA ligand is consistent with larger strain in the equatorial plane of uranyl with the former ligand, as pointed out in the text.

determines the coordination number CN of cation. In the case of alkali, alkaline earth, actinide, or lanthanide cations, for which dominant interactions with ligands are mostly electrostatic in nature and nondirectional, one might intuitively think that ligands progressively fill the first shell up to saturation before moving to the second shell. This is not so simple. In the case of the $\text{YbCl}_3(\text{CMPO})$ complex, it has been found that, in the gas phase, the CMPO ligand spontaneously moves from bidentate to monodentate coordination, despite the initially low CN of 5, presumably as a result of avoided intraligand strain and ligand/anion repulsions in the bidentate form.²³ This contrasts with the high CN of 12 found in the solid state structure of the $\text{Eu}(\text{NO}_3)_6^{3-}$ complex⁶³ which suffers high anion–anion repulsions. The possible effect of the surrounding medium on the CN in $\text{UO}_2(\text{OH})_4^{2-}$ and $\text{UO}_2\text{F}_4(\text{OH}_2)^{2-}$ complexes has been recently addressed.⁶⁴ In the case of Na^+ hydration, QM calculations⁶⁵ and molecular dynamics simulations on $\text{Na}(\text{OH}_2)_n^+$ aggregates⁶⁶ indicate that CN is not a simple intrinsic property of the first shell of the cation, but depends on second shell and long range effects and temperature, which likely contribute to the mono- versus bidentate coordination mode of bifunctional ligands as well.⁶⁷ On the computational side, further insights into the mono- versus bidentate coordination in solution could be obtained from free energy perturbation calculations along a suitable pathway^{68,69} using, e.g., Car Parrinello Molecular Dynamics to account for the electronic reorganization that takes place in the process.⁷⁰

4.3. On the Preference for 6- versus 7-Chelate Ring Complexes with Uranyl Salts. The question of preferred chelate ring size appears to be intimately related to the “steric effects” in the first coordination shell. Indeed, according to our calculations, the 7-chelating ligand forms stronger complexes than the 6-chelating ligand in unsaturated or unstrained complexes, while in the strained $\text{UO}_2(\text{NO}_3)_2\text{L}$ and $\text{UO}_2\text{L}_3^{2+}$ bidentate complexes, the two types of ligands have similar binding energies and the $\text{UO}_2\text{L}_3^{2+}$ cannot accommodate three bidentate AccA ligands. There are no related experimental data in the gas phase while, in solution, opposite trends are generally accepted and the chelate effect decreases with larger rings.^{5,6} Examples of lanthanide and uranyl complexes with dioxygen ligands have been given in the

Introduction. In the solid state, there is some hint for the higher stability of 6-chelating diamides: malonamides²⁶ and succinamides²⁷ display chelate coordination (exceptions can be found when they bind two metals simultaneously^{71,72}), while glutaramides are only monodentate.⁷³ The preference for small chelating rings in lanthanide complexes has been attributed to the higher steric strain with the larger ligand, where higher strain was inferred from somewhat larger $\text{C}=\text{O}$ –metal angles.¹² Our calculations on the uranyl and lanthanide²³ complexes do not support this interpretation, as enlargement of $\text{C}=\text{O}$ –metal angles is per se stabilizing.

Other contributions may come from the environment effect on ligand binding energies. As already discussed, immersing the complex from the gas phase into a cavity surrounded by a polarizable dielectric medium perturbs markedly the bond lengths and should perturb the corresponding binding energies as well. It is, however, difficult to provide some estimation of this effect. Changes in ligand solvation energies when moving from the uncomplexed to the complexed structure depend on the ligand size.⁷⁴ The role of substituents may be another matter of concern, in relation to changes in oxygen basicities⁷⁵ and to steric effects leading to restricted conformational freedom. As discussed in the preceding section, the entropy cost for immobilizing longer ligands is higher for shorter ligands, thus following trends observed in solution for uranyl or lanthanide cation complexes.^{8,9,12} In solution, the contributions of ligand conformational changes and other (mainly solvation) effects to the $\Delta\Delta S$ components remain, however, to be assessed.²⁰

Deeper insights into the ring size selectivity could be obtained from gas phase data, but these are not available for the simulated systems. Gas phase studies of diamine ligand coordination to a nickel complex show that a 5-chelating ligand is preferred over a 6-chelating one, due to the enthalpy, compensated by a large positive entropy.^{3,76} Moving to smaller metals and smaller coordination numbers shifts the preference for 6-membered chelate rings. For this class of complexes, there seems to be consensus on the enthalpic origin of the chelate ring size effect.⁴ The metal–ligand bonds with uranyl are less “covalent” and directional than with first row transition metals and involve harder interactions and higher coordination numbers. It is thus unclear whether the origin of the ring size effect can be extended to actinide and lanthanide complexes.

4.4. Comparison of Bidentate Diamide versus Bis-Monoamide Uranyl Complexes. According to the isodesmic

(63) Zhang, L.; Zhou, Y.; Xu, L.; Yu, Z.; Razak, I. A.; Chantrapromma, S.; Fun, H.-K.; You, X. *Inorg. Chem. Commun.* **2001**, *4*, 368.

(64) Vallet, V.; Wahlgren, U.; Schimmelpennig, B.; Moll, H.; Szabo, Z.; Grenthe, I. *Inorg. Chem.* **2001**, *40*, 3516–3525.

(65) Derepas, A. L.; Soudan, J. M.; Brenner, V.; Dognon, J. P.; Millié, P. *J. Comput. Chem.* **2002**, *23*, 1013–1030.

(66) Brodskaya, E.; Lyubartsev, A. P.; Laaksonen, A. *J. Chem. Phys.* **2002**, *116*, 7879–7892.

(67) If the ring size and chelate effects are not of enthalpic origin, they can hardly be interpreted in terms of strain or stresses of the ligands. Great care should thus be taken in overinterpreting small structural changes (e.g., in bite angles or in metal–O=C angles) as a result of preferred chelate ring size. Generally, large deformation of the ligands may be indicative of stronger interactions with the metal. As shown in our analysis, changes in structural parameters intrinsically depend on the chelate ring size, counterions, and stoichiometry.

(68) Beveridge, D. L.; DiCapua, F. M. *Annu. Rev. Biophys. Biophys. Chem.* **1989**, *18*, 431–492.

(69) Jorgensen, W. L.; Buckner, J. K. *J. Phys. Chem.* **1987**, *91*, 6083–6085.

(70) Marx, D.; Tuckerman, M. E.; Hutter, J.; Parrinello, M. *Nature* **1999**, *397*, 601–604 and references therein.

(71) Kannan, S.; Ferguson, G. *Inorg. Chem.* **1997**, *36*, 1724–1725.

(72) Mistryukov, V. E.; Mikhailov, Y. N. *Koord. Khim.* **1983**, *9*, 97.

(73) Charpin, P.; Lance, M.; Nierlich, M.; Vigner, D.; Charbonnel, M.-C.; Musikas, C. *Acta Crystallogr.* **1987**, *C43*, 442–445.

(74) Using the GB-SA solvation model implemented in the MACRO-MODEL software and the corresponding AMBER* atomic charges, we calculated the hydration energies of AccA and AcA, taking their QM optimized structures within the bidentate and monodentate $\text{UO}_2(\text{NO}_3)_2\text{L}$ complexes. AcA was found to be better hydrated than AccA (by 5 kcal/mol for the bidentate ligands and by 3 kcal/mol for the monodentate ligands).

(75) Spjuth, L.; Liljenzin, J. O.; Hudson, M. J.; Drew, M. G. B.; Iveson, P. B.; Madic, C. *Solvent Extr. Ion Exch.* **2000**, *18*, 1–23.

(76) Emmenegger, F.; Schlaepfer, C. W.; Stoekli-Evans, H.; Piccand, M.; Piekarski, H. *Inorg. Chem.* **2001**, *40*, 3884–3888.

reaction modeling the exchange of one bidentate diamide L for two monoamide ligands A, the latter are enthalpically preferred in the gas phase. There are a number of possible reasons for that: (i) The bidentate coordination requires a conformational change of L from *trans* or *gauche* to *cis* which induces internal strain, partly due to the “parallel” arrangement of the O=C dipoles. We notice that the ligand deformation energies ΔE_{def} of $L_{\text{bidentate}}$ (10–13 kcal/mol) contribute to more than 50% of the ΔE_{iso} energies. These calculated values are lower estimates of the “real” deformation energies, as they do not take into account the polarization of the O=C dipoles by uranyl, which would lead to stronger dipole–dipole repulsions than those in the electronically relaxed ligands. In the case of conformationally locked bifunctional *cis* ligands, such strain is not to be paid upon complexation.⁷⁷ (ii) The bidentate ligand cannot achieve optimal binding for its two binding sites. This can be seen from the optimized U–O distances (they are ≈ 0.1 Å longer in the bidentate than in the bis-monodentate complexes),⁷⁸ or from the U–O=C angles (they are ≈ 20 – 30° smaller in the bidentate than in the monodentate ligand, leading to reduced polarization of the $O^\delta-C^\delta+$ bonds; see Tables S6 and S8). (iii) Anion–anion repulsions are less important in bis-monodentate complexes (X–U–X angle = 180°) than in the bidentate complex (X–U–X $\approx 120^\circ$; see Table 3 and S11). (iv) Steric crowding in the equatorial plane of uranyl is larger with bidentate than with monodentate ligands and larger with NO_3^- than with Cl^- counterions, in relation to the shorter $\text{O}(\text{NO}_3)\cdots\text{O}(\text{NO}_3)$ contacts (2.64 Å in the bidentate AccA complex and 2.71 Å in the AcA bidentate complex), compared to the $\text{Cl}\cdots\text{Cl}$ distances (4.34 Å and 4.36 Å, respectively). Steric crowding in the equatorial plane of uranyl is also larger with AccA than with AcA, as seen from the X–U–X angles, which are somewhat smaller with the former ligands, as observed in the corresponding solid state structures.^{26,27} These conclusions are unlikely to be altered if the contributions of vibrational free energies are taken into account. Differences in entropy changes for immobilizing one diamide L ligand versus two monoamide

(77) Lumetta, G.; Rapko, B. M.; Garza, P. A.; Hay, B. P.; Gilbertson, R. D.; Weakly, T. J. R.; Hutchinson, J. E. *J. Am. Chem. Soc.* **2002**, *124*, 5644–5645.

(78) X-ray structures of uranyl nitrate with amide ligands display the same trend. Compare, for instance, the DOGZOO, FEPFAH, HALFUV, and FETIH structures of complexes with two monodentate ligands and the XEVNAN complex with the AccA bidentate ligand. The REFCODES are from the Cambridge Crystallographic Structural Database.

A ligands in the gas phase are likely to be smaller than the calculated ΔE_{reac} energies, which leads us to conclude that, in the gas phase, there is no preference for chelating coordination of diamide ligands to uranyl salts.

There are, to our knowledge, no thermodynamic data on diamide versus monoamide complexation, in solution, but it is accepted that diamides extract lanthanide or actinide cations more efficiently than monoamide analogues do.⁷⁹ Again, the contrasted conclusions drawn from static structures in the gas phase and from experimental results in solution point to the role of environment and dynamics. Entropy effects are expected to play a major role, as in the case of lanthanide ion complexation.^{9,10,12,14,20} This is consistent with our results, according to which there is no intrinsic (gas phase) enthalpic preference for chelation in saturated complexes, but the solvent contributions to both enthalpy and entropy components remain to be clarified.⁸⁰ Beyond the studied diamide systems, the question of chelating coordination as a function of metal, nature of binding sites, ring size, and counterions also has bearing on bifunctional ligands (CMPO, diphosphine oxide, picolinamide, polycarboxylate) grafted onto organized rigid platforms such as calixarene or resorcinarenes,^{81,82} where the cation binding mode also relates to the hydrophobicity and extractability of the formed complex.

Acknowledgment. The authors are grateful to CNRS, IDRIS, CINES, and Université Louis Pasteur for computer resources and to PRACTIS and EEC (Contract F1KW-CT-2000-0088) for support. G.W. thanks Professor C. Madic for stimulating discussions.

Supporting Information Available: Additional figures and tables. This material is available free of charge via the Internet at <http://pubs.acs.org>.

IC0341082

(79) Byers, P.; Drew, M. G. B.; Hudson, M. J.; Isaacs, N. S.; Madic, C. *Polyhedron* **1994**, *13*, 349. Siddall III, T. H.; Good, M. L. *J. Inorg. Nucl. Chem.* **1967**, *29*, 149–158; Charbonnel, M.-C. *PhD Thesis*, Clermond-Ferrand, 1988.

(80) For instance, in the case of ditopic flexible ligand binding to cyclodextrins in water, the chelate type complex is favored by enthalpy, not by entropy (Breslow, R.; Belvedere, S.; Gershell, L.; Leung, D. *Pure Appl. Chem.* **2000**, *72*, 333–342).

(81) Böhmer, V. In *Calixarenes for Separation*; Lumetta, G., Rogers, R., Gopalan, A., Eds.; ACS Symposium Series 757; ACS: Washington, DC, 2000; pp 135–148.

(82) Boerrigter, H.; Verboom, W.; Reinhoudt, D. N. *J. Org. Chem.* **1997**, *62*, 7148–7155.